

Multiplex Screening of Protein Glycosylation Using Lectin-Binding Biophotonic Microarray Imaging

Martin J. Weissenborn,^a Rouslan V. Olkhov,^b Sabine L. Flitsch,^a Andrew M. Shaw^{b}*

^a School of Chemistry & MIB, The University of Manchester, Manchester, M1 7DN, United
Kingdom

^b College of Life and Environmental Sciences, University of Exeter, Exeter, EX4 4QD, United
Kingdom

KEYWORDS: protein glycosylation, posttranslational modification (PTM), lectin, microarray
imaging

ABSTRACT

Lectin binding with tethered monosaccharides has been studied using the particle plasmon light-scattering properties of gold nanoparticles printed into an array format. Aminoethyl-functionalised monosaccharides were printed onto self-assembled monolayers of hydroxyl- and carboxyl-groups. A detailed analysis of the binding of concanavalin A (ConA) and wheat germ agglutinin (WGA) to their target sugars indicate affinity constants in the order of $K_D \sim 10$ nM for the presented monosaccharides. The detection limits for the lectins following a 200 seconds injection time were determined as 10 ng/ml or 0.23 nM and 100 ng/ml or 0.93 nM, respectively.

An eight-lectin screen was performed on the glycoprotein pig fibrinogen (FBR). Four lectins showed specific binding with a spectrum of K_D values similar in magnitude to the tethered-sugar-lectin interactions. The array technology has potential to perform a multi-lectin screen of large numbers of proteins in 200 seconds providing information on protein glycosylation and their micro-heterogeneity.

INTRODUCTION

The analysis of protein glycosylation has become an important facet of biopharmaceutical production as glycoproteins make up more than one third of approved biopharmaceuticals [1-3](#). For glycoprotein hormones, such as human erythropoietin, glycosylation determines pharmacokinetic and pharmacodynamic profiles [4-5](#). The plethora of therapeutic antibodies currently in the clinic and development need to be expressed with precise glycosylation patterns for correct therapeutic function [6](#). Given the dynamic character of glycosylation during and after protein translation in the cell, tight quality control of biopharmaceutical production is needed with fast, efficient and precise analytical techniques to monitor protein glycosylation.

Glycosylation is the most abundant post-translational modification (PTM) in nature, where glycans are attached to proteins or lipids [7](#). The glycosylation is highly diverse and is therefore used as a unique pattern for cell-cell recognition [8](#). Protein glycosylation is important for the refolding, solubility and stability of the proteins [9](#), and defects in glycosylation are observed in diseases such as allergies or muscular dystrophies [10-11](#). The determination and detection of different glycosylation is non-trivial, laborious and requires a complex set of analytical techniques [12](#). Amongst them are nuclear magnetic resonance [13](#), mass spectrometry [14](#) in combination with gas and liquid chromatography [15](#), and eastern or lectin blotting [16-17](#). An important tool for characterising glycans is the specific binding of lectins, which are

commercially available and can be highly selective for mostly terminal saccharides [18-21](#). In combination with surface plasmon resonance (SPR) [22](#), lectins can provide useful quantitative data on protein glycosylation without the need for the more conventional fluorescent labelling of probes [21, 23](#). Using the SPR label-free technology in an array format allows the study of a large numbers of carbohydrate-protein interactions including determination of binding kinetics, affinity and avidity constants and relative energies of interactions.

We have developed an SPR related label free biophotonic sensor array technique [24](#) for the analysis of proteins from solution including antibodies from complex fluids [25](#). The technique uses the sensitivity of the light scattering properties of the gold nanoparticle localised surface plasmons to provide intensity changes observed in real time with a video camera. The gold nanoparticle array spots can be functionalised by self-assembling monolayers (SAMs) which carry a terminal carboxylic group (linker) for chemical modification and a terminal hydroxyl group (spacer), respectively [26-27](#). The carboxylic group can be used to couple various different chemically modified sugars on the surface [28](#). The hydroxyl group carrying molecule spacer allow spacer dilutions, which is important to understand the different affinities of lectins to high and low concentrated sugars on the surface [29-30](#). Also larger molecules, such as glycoproteins, can be coupled into the SAMs and their glycosylation can be studied.

Here, we report the first analysis for the label-free biophotonic imaging detection of glycans on the glycoprotein fibrinogen. For proof-of-principle studies, the lectin binding specificities and its kinetics were studied using monosaccharide standards galactose (Gal), mannose (Man), glucose (Glc) and *N*-acetylglucosamin (GlcNAc), which were analysed with eight different lectins. The surface concentration of each sugar was varied to assess the effect on the association and dissociation kinetics and hence differential lectin affinity for the sugars. The optimised protocols

were subsequently applied to the protein fibrinogen using bovine serum albumin as a negative control, where four different lectins showed binding affinity towards fibrinogen. This new technique enables the fast screen of protein glycosylation and could therefore become valuable in the quality control of glycosylated biopharmaceuticals.

EXPERIMENTAL METHODS

Reagents. Self-assembling monolayer (SAM) components: HS-(CH₂)₁₇-(OC₂H₄)₃-OH (used as a ‘spacer’) and HS-(CH₂)₁₇-(OC₂H₄)₆-OCH₂COOH (used as a ‘linker’), were obtained from ProChimia Surfaces (Poland). *N*-(3-dimethylaminopropyl)-*N'*-ethylcarbodiimide hydrochloride (EDC), *N*-hydroxysuccinimide (NHS), bovine serum albumin (BSA), fibrinogen fraction I from pig plasma (FBR), were obtained from Sigma-Aldrich. The lectins erythrina cristagalli (ECA), lens culinaris (LcH), galanthus nivalis (GNA), arachis hypogaea (peanut) (PNA), sambucus nigra (SNA), and aleuria aurantia (AAL) were kindly provided by Galab (Germany) as 1 mg/ml solutions in Tris buffer. The concanavalin A (ConA), and wheat germ (WGA) lectins were acquired from Vector labs as 5 mg/mL solution in HEPES buffer. All lectins were supplied FITC tagged. The standard running and dilution buffer was phosphate buffered saline (0.01 M phosphate buffer, 0.0027 M potassium chloride and 0.137 M sodium chloride, pH 7.4), containing 5×10⁻⁵ w/w Tween 20 surfactant, PBST. Aqueous 100 mM phosphoric acid solution, pH 1.9, was used as the regeneration buffer.

Aminoethyl glycoside derivatives of the monosaccharides α-D-mannose (Man), β-D-glucose (Glc), β-D-galactose (Gal), and *N*-acetyl-β-D-glucosamine (GlcNAc) were prepared by glycosylation methods reported elsewhere [28](#).

Sensor array preparation. The manufacture of the gold nanoparticle biophotonic arrays used in these experiments are described in detail elsewhere [24, 31](#). Briefly, the rectangular 12 × 8 sensor

arrays are inkjet printed with a 300 μm pitch between the spots and a spot diameter of 200 μm , Figure 1. Each spot is printed with seed nanoparticles 4 nm in diameter, removed from the printer and placed in growth solution to grow truncated polyhedral gold nanoparticles with an approximate diameter of 120 nm. These particles are present with a surface density of approximately 25% and are the plasmon light-scattering centres for assays. The arrays are then returned to the inkjet printer to prepare the assays.

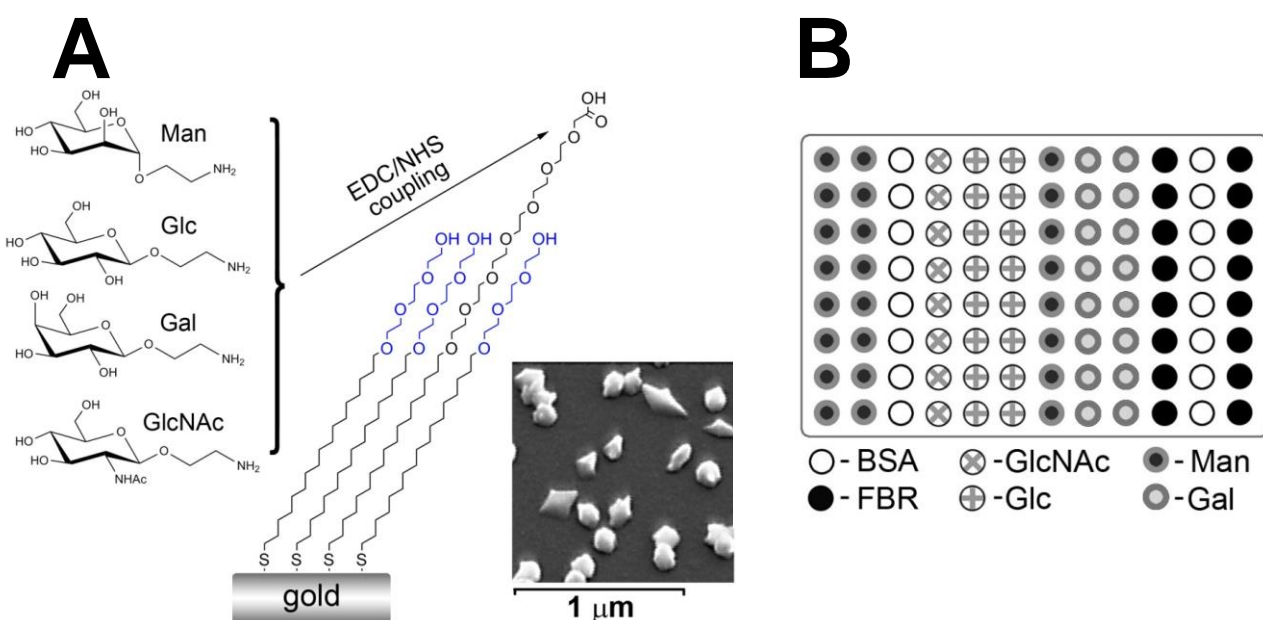


Figure 1. Sensor preparation details: (A) monosaccharides used to functionalise sensor arrays by EDC/NHS coupling to carboxylic groups present in self-assembling monolayers (SAMs) (left). The hydroxyl and carboxy terminal molecules form the SAMs on gold nanoparticles shown in SEM image (right); (B) Array print legend.

Analyte binding specificity is introduced by functionalisation of the gold surface with a particular monosaccharide or a protein. Before the functionalisation the sensor surface was activated by coating the gold nanoparticles with a mixed SAM of linker and spacer molecules, Figure 1A, followed by activation of the linker carboxylic groups with the common EDC/NHS

chemistry to produce succinimide esters reactive towards primary amino groups. Five mixtures with different ratios of linker to spacer SAM components were used: 1:4, 1:10, 1:100, 1:1000, and 1:2500.

Four monosaccharides, mannose (Man), galactose (Gal), glucose (Glc), and *N*-acetylglucosamine (GlcNAc), and two proteins, bovine serum albumin (BSA), and human fibrinogen (FBR) were inkjet printed onto activated sensors according to the legend shown in Figure 1B, incubated overnight at room temperature, rinse washed with deionised (DI) water, and stored at 4 °C until used.

Lectin binding kinetic assay. The sensor arrays are re-hydrated in PBST buffer for 15 minutes, washed with regeneration buffer, blocked with 2 mg/ml solution of BSA in PBST for 10 minutes, washed again with regeneration buffer and finally stabilised in PBST running buffer flow. An injection of doubly concentrated PBS buffer was performed to establish the sensitivity of the array spots to the change of an analyte bulk refractive index, these data were used to convert relative brightness response into a scale equivalent to refractive index change, conventionally this is given in response units, RU ($\text{RU} \equiv 10^{-6}$ refractive index units ³²). The sensitivity of each array spot is typically 8×10^{-5} RIU and the assays are averaged over 8 or 16 spots as required for multiplexed results.

A typical binding experiment procedure is shown in Figure 2A: (i) the baseline plasmon scattering intensity is recorded in the flow of running PBST buffer; (ii) the lectin sample solution was injected over the surface for approximately 200 s to record the association binding phase with sufficient accuracy to determine the association rate constant, k_a ; (iii) the flow was switched to running buffer and dissociation phase kinetics were recorded for approximately 10 minutes; and (iv) the sensor was regenerated with 100 mM phosphoric acid solution.

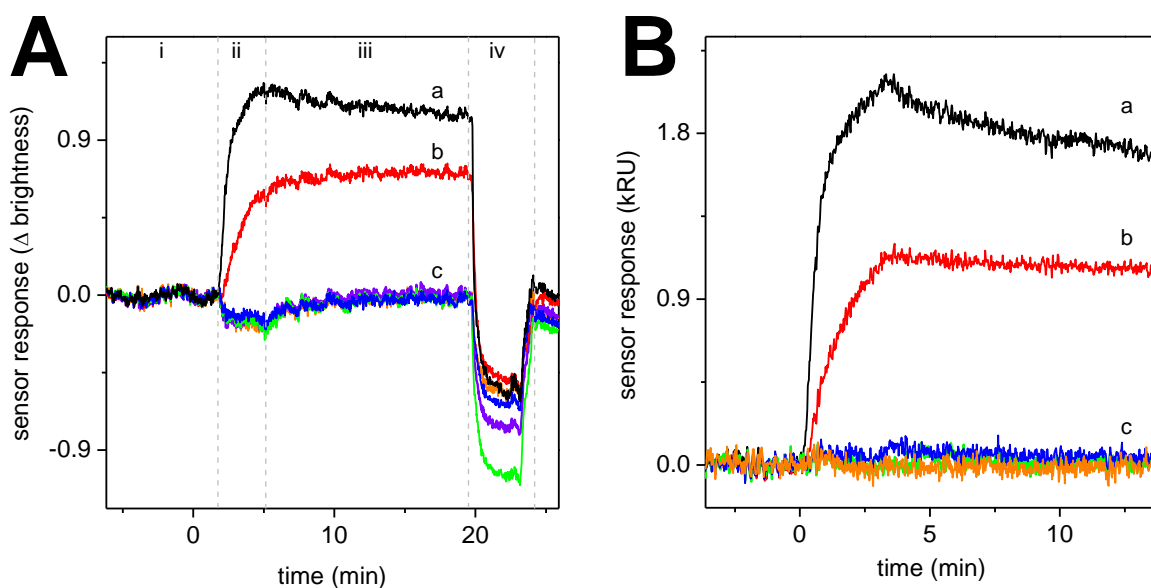


Figure 2. Example of the experimental sensogram data recorded in an assay of 2 $\mu\text{g}/\text{mL}$ ConA lectin sample: (A) averaged scattering intensity changes recorded from 8 or 16 arrays spots functionalised with the same material showing the experimental phases (i) baseline, (ii) association, (iii) dissociation, (iv) regeneration; (B) Data from panel A is referenced against the BSA control channels to compensate for the differences in refractive indices of running buffer and lectin samples. The control channel further corrects for temperature variations and light source intensity instabilities. The signal scale is converted into response units and injection time lag removed. The marked traces on both panels are: a – Man, b – FBR, and overlapping c – Gal, Glc, GlcNAc, and BSA (panel A only).

The regeneration step (iv) removes the adsorbed analyte material from the assay spot and allows the array to be re-used two or three times without loss of sensitivity or specificity. This allows assays to be repeated several times on the same sensor array without noticeable degradation in performance. The assay is repeated with several concentrations of the target

binding lectin and the kinetic data subjected to a global fit for all concentrations, both association and dissociation simultaneously for all concentration, from which the rate constants, k_a and k_d can then be determined. The variation with the rates with time for a simple 1:1 binding model is performed and deviations from this model may provide information on more complex interaction such as co-operative binding and avidity. Affinity and avidity constants can then be determined for all of the interactions. An example of the procedure is shown in Figure 2B with 2 $\mu\text{g/ml}$ of ConA which has a strong binding of the lectin to mannose and FBR functionalised sensor surfaces. The rest of the monosaccharide surfaces—Gal, Glc, and GlcNAc—do not show any affinity towards the ConA analyte. Qualitative comparison of the responses in Man and FBR channels revealed that although the rate of association with fibrinogen is slower the dissociation is also markedly slower than in Man the channel.

RESULTS

The Man and GlcNAc saccharides are known to bind selectively to ConA and WGA ³³, respectively. The specific binding interactions between the modified sugars printed onto the array with the lectins ConA and WGA were studied over a range of lectin concentrations. The concentration-dependence series of kinetic binding responses were globally fitted (simultaneously for all concentrations in association and dissociation) analysed with a 1:1 interaction model resulting in association and dissociation rate constants listed in Figure 3 and Table 1. The thermodynamic equilibrium dissociation constants K_D may then be derived from the fitted rate constants: $K_D = k_d/k_a$. The sensograms with lectin concentrations above 10 $\mu\text{g/ml}$ significantly deviate from the exponential functional form expected for a simple 1:1 binding model and were excluded from the global fit.

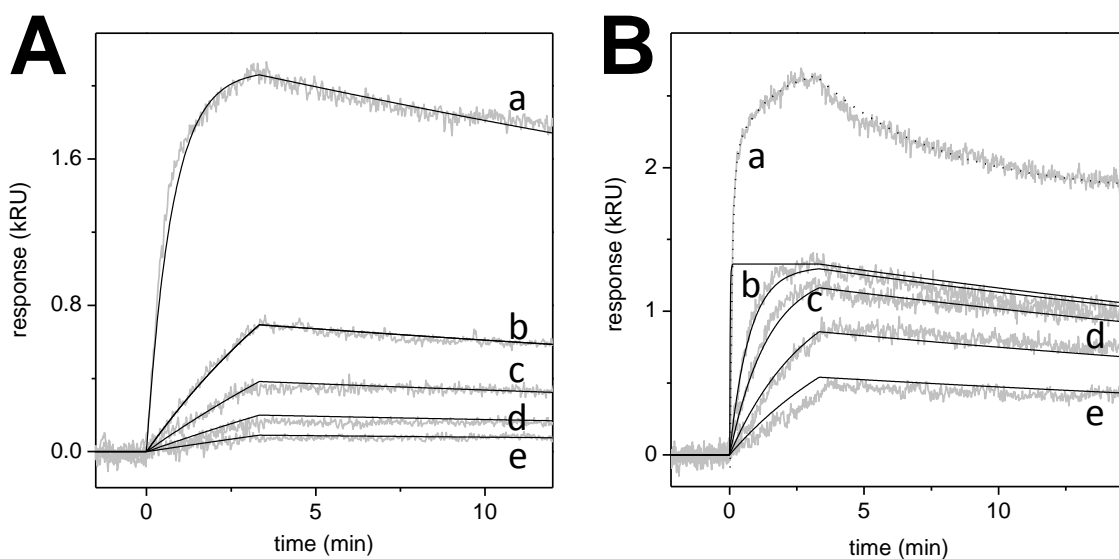


Figure 3. Global fit for all concentrations for the specific binding of the lectins to the surface-tethered sugars assuming a 1:1 interaction model: (A) ConA-Man binding with ConA concentrations (a) 24, (b) 2.3, (c) 1.2, (d) 0.57, (e) 0.25 $\mu\text{g/ml}$; (B) WGA-GlcNAc, with WGA concentrations (a) 48, (b) 1.2, (c) 0.62, (d) 0.30, (e) 0.15 $\mu\text{g/ml}$; kinetic trace (a) has a weighting of 10^{-5} in the global fit, solid curve, while the dotted curve corresponds to the individual fit of this trace to double exponential functions.

The strongest specific responses were observed for lectin-monosaccharide pairs of ConA-Man and WGA-GlcNAc shown in Figure 3 with their corresponding global fit analyses. For the lower concentrations of both lectins, the 1:1 binding model shows a good fit. At higher ConA concentrations, Figure 3A, the fit to the exponential function remains reasonable whereas there are significant deviations from the single exponential functional form for the WGA-GlcNAc pair, Figure 3B, indicating a departure from the 1:1 binding model. The kinetic response for 48 $\mu\text{g/ml}$ WGA appears to consist of faster and slower processes, the latter can be readily characterised if double exponential function was used to fit the data, resulting in the kinetic and

thermodynamic parameters of the slower process $k_a = (1.1 \pm 0.2) \times 10^4 \text{ s}^{-1} \text{ M}^{-1}$, $k_d = (3.7 \pm 0.1) \times 10^{-3} \text{ s}^{-1}$, $K_D = 346 \pm 55 \text{ nM}$, $\Delta G = 36.4 \pm 0.5 \text{ kJ M}^{-1}$.

Table 1. ConA-Man interaction rate constants observed on sensor surfaces with varying SAM linker:spacer ratios.

| linker :spacer | $10^{-4} \times k_a (\text{M}^{-1} \text{ s}^{-1})$ | $10^4 \times k_d (\text{s}^{-1})$ | $K_D (\text{nM})$ | $-\Delta G (\text{kJ M}^{-1})$ |
|----------------|---|-----------------------------------|-------------------|--------------------------------|
| 1:4 | 4±3 | 10±0.3 | 24±20 | 42.7±4.6 |
| 1:10 | 7.3±0.2 | 7.4±0.3 | 10±0.4 | 45.2±0.5 |
| 1:100 | 7.0±0.4 | 9.9±0.8 | 14±1.5 | 44.4±0.5 |
| 1:1000 | 9.7±0.1 | 3.2±0.1 | 3.3±0.1 | 47.7±0.5 |
| 1:2500 | 11.8±0.2 | 3.3±0.1 | 2.8±0.1 | 48.1±0.5 |

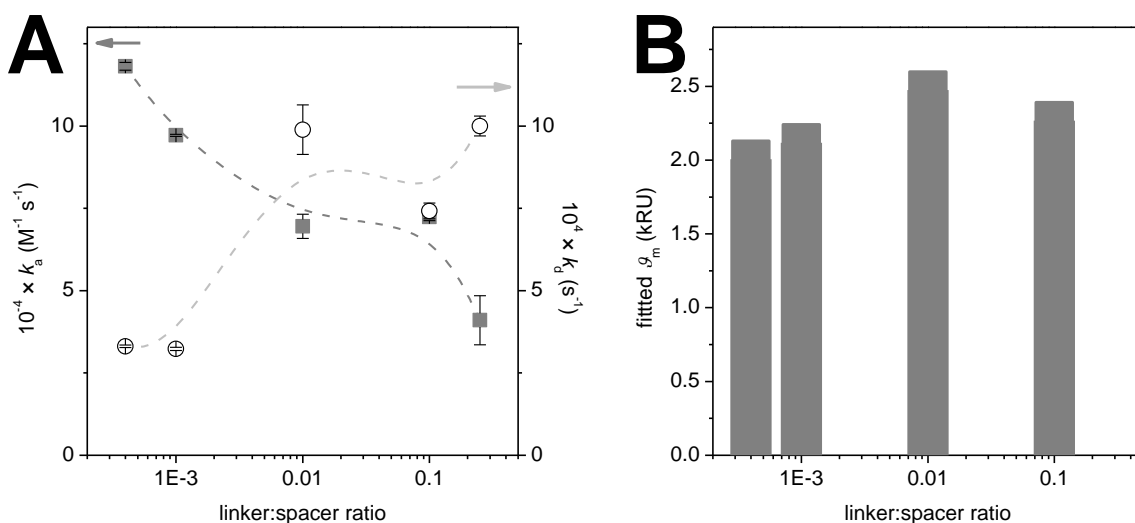


Figure 4. Dependence of kinetic parameters derived from the series of ConA-Man sensograms on the linker:spacer ratio: (A) association, filled squares, and dissociation, open circles, rate constants; (B) fitted values of maximum analyte surface coverage. It appears that smaller numbers of Man binding sites on the sensor surface leads to stronger specific binding of lectin molecules from the analyte solution to the sensor surface.

The sensitivity of the assays may be assessed for the 200 s injection time indicating a detection limit of 10 ng/ml or 0.23 nM for WGA and 100 ng/ml or 0.93 nM for ConA. These values compare favourably with other techniques, for example the bulk phase mannose glycol-conjugated nanoparticle based absorption and scattering measurements were shown to have ConA limits of detection 2-3 nM ³⁴.

The deviations from the 1:1 model indicated a more complex avidity interaction at high concentrations of lectin so we have performed a series of experiments to determine the variation of the kinetic and thermodynamic parameters for the interactions between the lectins and different densities of sugars on the surface. The sugar surface density was varied by varying the SAM composition by changing the linker:spacer ratio, Figure 4. This reduced the surface sugar density and the potential for multiple lectin-sugar interactions. The variation of the association and dissociation rate constants for the interactions is shown in Figure 4 and summarised in Table 1.

We observed significant binding to FBR compared to the BSA control channel during the experiments since FBR is *N*-glycosylated ³⁵. The data showed interactions of FBR with the lectins ConA and WGA, respectively. FBR was coupled to the SAMs in a 1000:1 linker:spacer dilution and was subsequently interrogated with six different lectins, Figure 5. The monosaccharides Glc, GlcNAc, Man and Gal were used as controls. The strong specific binding to FBR was observed for WGA and ConA, in addition specific binding was observed for SNA and LcH—which interact with sialic acid and a fucosylated core regions, respectively, Figure 5 and Figure 6.

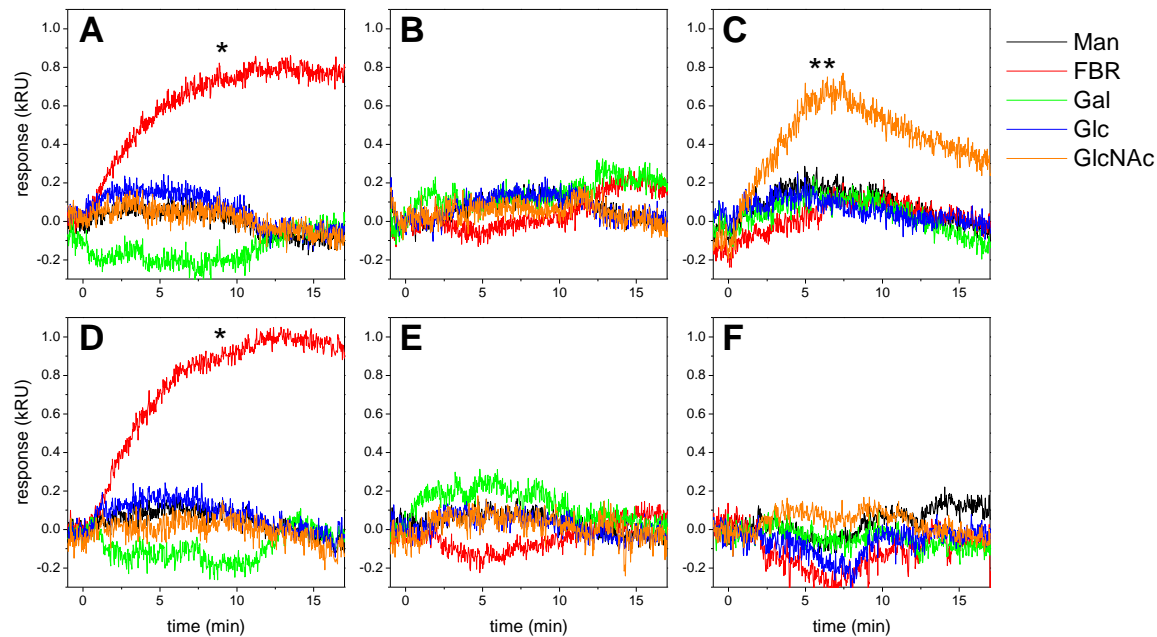


Figure 5. Binding assays of SNA (A), GNA (B), ECA (C), LcH (D), PNA (E), and AIL (F) lectins performed on sensors coated with 1:1000 linker:spacer SAMs. Each lectin sample was injected for ca. 10 minutes at 9.6 $\mu\text{g/ml}$ concentration. The SNA and LcH lectins showed a clear affinity towards the FBR surface (traces marked with * on panels A and D). ECA shows some affinity towards GlcNAc functionalised surfaces (marked ** on panel C).

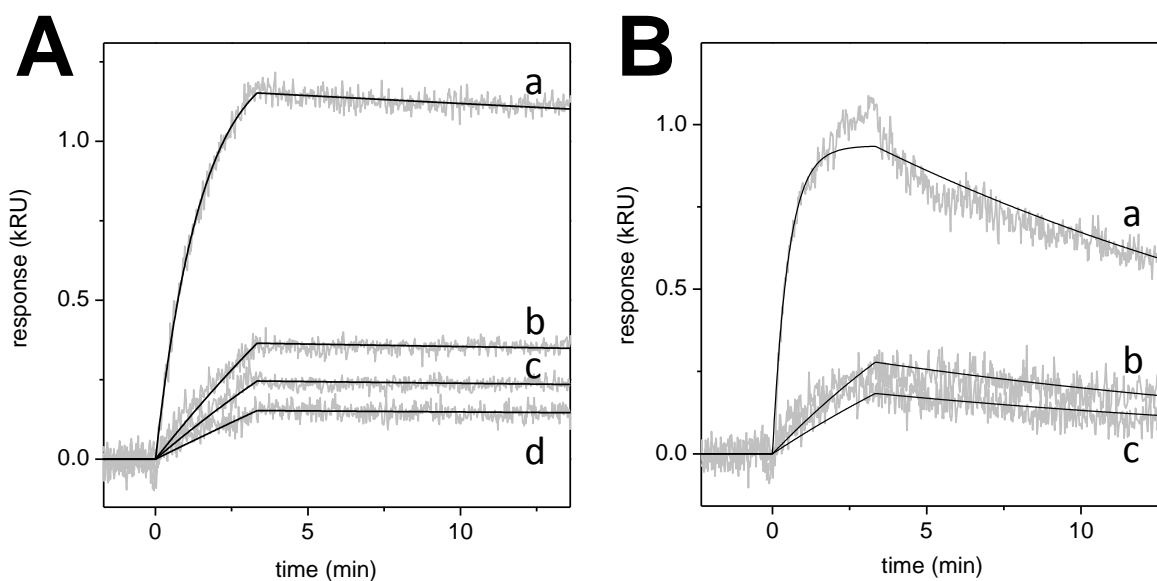


Figure 6. Kinetic analysis of lectin-FBR interaction. Response data were obtained on sensor arrays functionalised with SAMs of 1:1000 linker:spacer ratio. (A) ConA-FBR, lectin analyte concentrations were (a) 24, (b) 2.3, (c) 1.2, (d) 0.57 $\mu\text{g/ml}$. (B) WGA-FBR, lectin analyte concentrations were (a) 48, (b) 1.2, (c) 0.62 $\mu\text{g/ml}$.

DISCUSSION

The aim of the current work was to assess the potential of an array-based, label-free particle plasmon screening technology for the rapid assessment of the posttranslational modification of proteins, specifically glycosylation. The monosaccharide standards Glc, GlcNAc, Gal and Man aminoethyl glycosides were prepared as published elsewhere [28](#). The aminoethyl glycosides were coupled to the carboxyl groups in SAMs allowing the surface sugar concentration to be varied by varying the linker-spacer ratio. Lower sugar surface densities are expected to result in a smaller number of binding sites on the surface reflecting simple 1:1 lectin-sugar binding kinetics. The kinetic parameters in Table 1 indicate a trend to a consistent determination and reproducibility

especially in the dissociation rate constant, k_d and hence the determination in K_D and the energy of interaction, Figure 4A. The number of lectins bound to the surface, however, derived from the fitted surface coverage, θ_m in Figure 4B, showed variations of only 20%. The theoretical separation between any linker-spacer in the SAM is 0.45 nm ³⁶⁻³⁷ with the separations in a rectangular matrix changing with increasing dilution: 0.9, 1.4, 4.5, 14.2, and 22.5 nm for 1:4, 1:10, 1:100, 1:1000, 1:2500 respectively. The distance between saccharide binding pockets of ConA is about 7.0 ± 0.5 nm ³⁸, which is two-three fold less than ideal inter-linker distance. Although this may suggest that ConA would bind only one site for the linker:spacer ratios 1:1000 and 1:2500, the realistic SAM with randomly distributed linker molecules shall offer ample amount of closer spaced sugars and two-site binding is reasonable. Moreover there is the fluidity within the SAM and a lectin may recruit additional binding sugars once bound to the initial site on the surface. The trend with monovalent binding is consistent with the trends observed in Figure 4 indicating binding affinity constants and energies for the sugar-lectin interactions as shown in Table 2.

Table 2. Lectin-ligand interaction rate constants observed on sensor surface with linker:spacer ratio 1:1000.

| lectin-ligand | $10^4 \times k_a (\text{M}^{-1} \text{s}^{-1})$ | $10^4 \times k_d (\text{s}^{-1})$ | K_D (nM) | $-\Delta G$ (kJ M^{-1}) |
|---------------|---|-----------------------------------|---------------|-----------------------------------|
| ConA-FBR | 4.9 ± 0.1 | 0.7 ± 0.1 | 1.4 ± 0.2 | 49.8 ± 0.5 |
| WGA-FBR | 2.9 ± 0.1 | 8.2 ± 0.2 | 28 ± 1 | 42.7 ± 0.5 |
| SNA-FBR | 1.7 ± 0.1 | 0.91 ± 0.10 | 5.4 ± 0.7 | 46.8 ± 0.5 |
| LcH-FBR | 1.4 ± 0.1 | 1.55 ± 0.1 | 11 ± 1 | 45.1 ± 0.5 |
| WGA-GlcNAc | 78.2 ± 0.5 | 3.2 ± 0.1 | 4.1 ± 0.4 | 47.3 ± 0.5 |
| ECA-GlcNAc | 1.6 ± 0.2 | 13.4 ± 0.5 | 82.7 ± 11 | 40.1 ± 0.6 |

The kinetic parameters derived in this study reflect the binding of the lectin specifically to the tethered sugar moieties and non-specifically to the glycol spacer molecule which dominates the SAM composition. It has been observed previously that the measured interactions between lectins and sugars depends on whether the sugar or the lectin is immobilised on the sensor surface and on whether the sugars are monomers or oligomers ³⁹⁻⁴³. The derived ConA-Man interaction parameters listed in Table 1 indicate K_D in low nanomolar range consistent with the expected values for the sugar surface ³⁹. In addition, aggregation of the lectins has been observed at higher concentration observing multi-lectin binding to the tethered-sugar surfaces ³⁹ which is consistent with the Figure 3B for WGA binding to GlcNAc. The relevant dissociation constants K_D for tethered-lectin-(mannose containing saccharide) binding reported in thermodynamic studies are in the range of 50-770 μ M for mono and disaccharides ⁴⁴⁻⁴⁶, and up to 750 nM for more complex longer and branched oligosaccharides ⁴⁵.

Table 3. K_D (in nM) matrix of sugar-lectin interactions.

| | AAL | SNA | PNA | LcH | WGA | ConA | GNA | ECA |
|--------|-----|---------|-----|------|---------|---------|-----|---------|
| PFBR | | 5.4±0.7 | | 11±1 | 28±1 | 1.4±0.2 | | |
| BSA | | | | | | | | |
| Glc | | | | | | | | |
| GlcNAc | | | | | 4.1±0.4 | | | 82.7±11 |
| Gal | | | | | | | | |
| Man | | | | | | 3.3±0.1 | | |

The lectins specificity, Figure 5, indicates binding to the expected tethered-sugars with some notable exceptions and binding of a series of lectins to glycoprotein, pig FBR, Table 2 and Table 3. All interactions, whether for the tethered sugar presented in the SAM surface or the sugar

presented by the printed FBR protein, showed K_D values of ~ 10 nM, Figure 6. Similarly, large concentration effects were observed for WGA-FBR binding, Figure 6B, consistent with lectin clustering. The lectin binding screening for all six lectins may be summarised in the K_D matrix shown in Table 3. Only three of the lectins bound to their expected tethered-sugar moieties: ConA-Man, WGA-GlcNAc and ECA-GlcNAc but four lectins showed specific binding to FBR. LcH binds to FBR indicating the presence of a fucose core structure on the surface of the protein in the correct presentation for the sugar to interact with the binding site of the lectin ⁴⁷. Neither AAL nor LcH binding to the Gal tethered to the surface nor does LcH bind to the Man tethered to the surface. The nature of the interactions between the lectins and the presentation of the sugars both on the surface and as presented on the glycoprotein FBR is not the same and indicative of the glycosylation pattern on FBR in some way ³⁵. The lectins WGA and ConA require terminal Man and GlcNAc monosaccharides, respectively, for binding but binding may also occur to specific patterns of oligosaccharides. The terminal monosaccharides can always occur due to the microheterogeneity in the glycosylation ⁴⁸. Furthermore, the lectin SNA showed specific binding to sialic acid moieties on surface proteins including FBR ⁴⁹⁻⁵⁰ and LcH specific binding to fucosylated biantennary core region ³⁵.

CONCLUSIONS

Our biophotonic scattering array screening technique for interactions with tethered sugars with a series of eight lectins producing a set of K_D with values ~ 10 nM with the expected specificity. The presentation of tethered sugars within the SAMs may in part explain the lack of binding of lectins to known sugar targets. A lectin screen of the tethered protein pig FBR shows a pattern of lectin binding with K_D values showing significant differences from the single sugar binding. The arrays have potential to be a new high-throughput screening technology to determine pattern of

lectin binding for protein glycosylation and potentially from a detailed analysis of the K_D values, a pattern of the protein and potentially glycosylation micro heterogeneity. The new array-based high-throughput technology has the potential to screen glycosylation of proteins rapidly and could therefore become a valuable tool in pharmaceutical research and industry.

AUTHOR INFORMATION

Corresponding Author

* E-mail: andrew.m.shaw@exeter.ac.uk

ACKNOWLEDGEMENTS

The authors like to thank Dr Robert Sardzik for providing the aminoethyl galactose. This work was supported by the Royal Society (Wolfson Award to SLF), the European Commission's Marie Curie program which funded the EuroGlycoArrays ITN (MJW) and the EPSRC.

REFERENCES

- (1) Hourihane, J. O. B., *Pediatr. Clin. North Am.*, 2011, 58 (2), 445-458.
- (2) Jefferis, R., *Trends Pharmacol. Sci.*, 2009, 30 (7), 356-362.
- (3) Kayser, V.; Chennamsetty, N.; Voynov, V.; Forrer, K.; Helk, B.; Trout, B. L., *Biotechnology Journal*, 2011, 6 (1), 38-44.
- (4) Narhi, L. O.; Arakawa, T.; Aoki, K. H.; Elmore, R.; Rohde, M. F.; Boone, T.; Strickland, T. W., *J. Biol. Chem.*, 1991, 266 (34), 23022-23026.
- (5) Li, H. J.; d'Anjou, M., *Curr. Opin. Biotechnol.*, 2009, 20 (6), 678-684.

- (6) Jefferis, R.; Lefranc, M. P., *Mabs*, 2009, 1 (4), 332-338.
- (7) Shin, I.; Park, S.; Lee, M. R., *Chem-Eur J*, 2005, 11 (10), 2894-2901.
- (8) Hartmann, M.; Lindhorst, T. K., *Eur. J. Org. Chem.*, 2011, (20-21), 3583-3609.
- (9) Walsh, C. T.; Garneau-Tsodikova, S.; Gatto, G. J., *Angew. Chem. Int. Ed.*, 2005, 44 (45), 7342-7372.
- (10) Yoshida-Moriguchi, T.; Yu, L. P.; Stalnaker, S. H.; Davis, S.; Kunz, S.; Madson, M.; Oldstone, M. B. A.; Schachter, H.; Wells, L.; Campbell, K. P., *Science*, 2010, 327 (5961), 88-92.
- (11) Arnold, J. N.; Wormald, M. R.; Sim, R. B.; Rudd, P. M.; Dwek, R. A., In *Annu. Rev. Immunol.*, Annual Reviews: Palo Alto, 2007; Vol. 25, pp 21-50.
- (12) Wada, Y.; Azadi, P.; Costello, C. E.; Dell, A.; Dwek, R. A.; Geyer, H.; Geyer, R.; Kakehi, K.; Karlsson, N. G.; Kato, K.; Kawasaki, N.; Khoo, K. H.; Kim, S.; Kondo, A.; Lattova, E.; Mechref, Y.; Miyoshi, E.; Nakamura, K.; Narimatsu, H.; Novotny, M. V.; Packer, N. H.; Perreault, H.; Peter-Katalinic, J.; Pohlentz, G.; Reinhold, V. N.; Rudd, P. M.; Suzuki, A.; Taniguchi, N., *Glycobiology*, 2007, 17 (4), 411-422.
- (13) Slynko, V.; Schubert, M.; Numao, S.; Kowarik, M.; Aebi, M.; Allain, F. H. T., *J. Am. Chem. Soc.*, 2009, 131 (3), 1274-1281.
- (14) Morelle, W., *Curr. Anal. Chem.*, 2009, 5 (2), 144-165.
- (15) Antonopoulos, A.; North, S. J.; Haslam, S. M.; Dell, A., *Biochem. Soc. Trans.*, 2011, 39, 1334-1340.
- (16) Tanaka, H.; Fukuda, N.; Shoyama, Y., *J. Agric. Food. Chem.*, 2007, 55 (10), 3783-3787.

- (17) Oguri, S., *Glycoconjugate J.*, 2005, 22 (7-9), 453-461.
- (18) Weissenborn, M. J.; Castangia, R.; Wehner, J. W.; Sardzik, R.; Lindhorst, T. K.; Flitsch, S. L., *Chem. Commun.*, 2012, 48 (37), 4444-4446.
- (19) Lis, H.; Sharon, N., *Chem. Rev.*, 1998, 98 (2), 637-674.
- (20) Šardžík, R.; Green, A. P.; Laurent, N.; Both, P.; Fontana, C.; Voglmeir, J.; Weissenborn, M. J.; Haddoub, R.; Grassi, P.; Haslam, S. M.; Widmalm, G.; Flitsch, S. L., *J. Am. Chem. Soc.*, 2012, 134 (10), 4521-4524.
- (21) Blixt, O.; Head, S.; Mondala, T.; Scanlan, C.; Huflejt, M. E.; Alvarez, R.; Bryan, M. C.; Fazio, F.; Calarese, D.; Stevens, J.; Razi, N.; Stevens, D. J.; Skehel, J. J.; van Die, I.; Burton, D. R.; Wilson, I. A.; Cummings, R.; Bovin, N.; Wong, C. H.; Paulson, J. C., *Proc. Natl. Acad. Sci. U. S. A.*, 2004, 101 (49), 17033-17038.
- (22) Karamanska, R.; Clarke, J.; Blixt, O.; MacRae, J. I.; Zhang, J. Q. Q.; Crocker, P. R.; Laurent, N.; Wright, A.; Flitsch, S. L.; Russell, D. A.; Field, R. A., *Glycoconjugate J.*, 2008, 25 (1), 69-74.
- (23) Voglmeir, J.; Sardzik, R.; Weissenborn, M. J.; Flitsch, S. L., *Omics*, 2010, 14 (4), 437-444.
- (24) Olkhov, R. V.; Shaw, A. M., *Biosens. Bioelectron.*, 2008, 23, 1298-1302.
- (25) Jansen van Vuuren, B.; Read, T.; Olkhov, R. V.; Shaw, A. M., *Anal. Biochem.*, 2010, 405 (1), 114-120.

- (26) Ostuni, E.; Chapman, R. G.; Holmlin, R. E.; Takayama, S.; Whitesides, G. M., *Langmuir*, 2001, 17 (18), 5605-5620.
- (27) Laurent, N.; Haddoub, R.; Voglmeir, J.; Wong, S. C.; Gaskell, S. J.; Flitsch, S. L., *ChemBioChem*, 2008, 9 (16), 2592-2596.
- (28) Sardzik, R.; Noble, G. T.; Weissenborn, M. J.; Martin, A.; Webb, S. J.; Flitsch, S. L., *Beilstein J Org Chem*, 2010, 6, 699-703.
- (29) Kiessling, L. L.; Splain, R. A., *Annu. Rev. Biochem*, 2010, 79, 619-653.
- (30) Gestwicki, J. E.; Cairo, C. W.; Strong, L. E.; Oetjen, K. A.; Kiessling, L. L., *J. Am. Chem. Soc.*, 2002, 124 (50), 14922-14933.
- (31) Olkhov, R. V.; Fowke, J. D.; Shaw, A. M., *Anal. Biochem.*, 2009, 385, 234-241.
- (32) Biacore User Training Documentation. GE Healthcare.
- (33) Bains, G.; Lee, R. T.; Lee, Y. C.; Freire, E., *Biochemistry*, 1992, 31 (50), 12624-12628.
- (34) Watanabe, S.; Yamamoto, S.; Yoshida, K.; Shinkawa, K.; Kumagawa, D.; Seguchi, H., *Supramol. Chem.*, 2011, 23 (3-4), 297-303.
- (35) Kollman, J. M.; Pandi, L.; Sawaya, M. R.; Riley, M.; Doolittle, R. F., *Biochemistry*, 2009, 48 (18), 3877-3886.
- (36) Bareman, J. P.; Klein, M. L., *J. Phys. Chem.*, 1990, 94 (13), 5202-5205.
- (37) Love, J. C.; Estroff, L. A.; Kriebel, J. K.; Nuzzo, R. G.; Whitesides, G. M., *Chem. Rev.*, 2005, 105 (4), 1103-1169.

- (38) Sanders, D. A. R.; Moothoo, D. N.; Raftery, J.; Howard, A. J.; Helliwell, J. R.; Naismith, J. H., *J. Mol. Biol.*, 2001, 310 (4), 875-884.
- (39) Duverger, E.; Frison, N.; Roche, A.-C.; Monsigny, M., *Biochimie*, 2003, 85 (1), 167-179.
- (40) Shinohara, Y.; Sota, H.; Kim, F.; Shimizu, M.; Gotoh, M.; Tosu, M.; Hasegawa, Y., *J. Biochem.*, 1995, 117 (5), 1076-1082.
- (41) Khan, M. I.; Sastry, M. V.; Surolia, A., *J Biol Chem*, 1986, 261 (7), 3013-3019.
- (42) Shinohara, Y.; Kim, F.; Shimizu, M.; Goto, M.; Tosu, M.; Hasegawa, Y., *Eur. J. Biochem.*, 1994, 223 (1), 189-194.
- (43) Dai, Z.; Kawde, A.-N.; Xiang, Y.; La Belle, J. T.; Gerlach, J.; Bhavanandan, V. P.; Joshi, L.; Wang, J., *J. Am. Chem. Soc.*, 2006, 128 (31), 10018-10019.
- (44) Houseman, B. T.; Mrksich, M., *Chem. Biol.*, 2002, 9 (4), 443-454.
- (45) Mandal, D. K.; Kishore, N.; Brewer, C. F., *Biochemistry*, 1994, 33 (5), 1149-1156.
- (46) Schwarz, F. P.; Puri, K. D.; Bhat, R. G.; Surolia, A., *J. Biol. Chem.*, 1993, 268 (11), 7668-7677.
- (47) Serna, S.; Yan, S.; Martin-Lomas, M.; Wilson, I. B. H.; Reichardt, N. C., *J. Am. Chem. Soc.*, 2011, 133 (41), 16495-16502.
- (48) Harmon, B. J.; Gu, X.; Wang, D. I. C., *Anal. Chem.*, 1996, 68 (9), 1465-1473.

(49) Pacchiarotta, T.; Hensbergen, P. J.; Wuhrer, M.; van Nieuwkoop, C.; Nevedomskaya, E.; Derks, R. J. E.; Schoenmaker, B.; Koeleman, C. A. M.; van Dissel, J.; Deelder, A. M.; Mayboroda, O. A., *J. Proteomics*, 2012, 75 (3), 1067-1073.

(50) Wu, P. G.; Lee, K. B.; Lee, Y. C.; Brand, L., *J. Biol. Chem.*, 1996, 271 (3), 1470-1474.

For TOC only:

